CARBON NANOTUBE MATERIALS FOR HYDROGEN STORAGE

A.C. Dillon, K.E.H. Gilbert, J. L. Alleman, T. Gennett, K.M. Jones, P.A. Parilla, and M.J. Heben
National Renewable Energy Laboratory
Golden, CO 80401-3393

Abstract

Carbon single-wall nanotubes (SWNTs) are capable of adsorbing hydrogen quickly, to high density, at ambient temperatures and pressures. Last year, we presented the details of a new SWNT cutting procedure that enabled hydrogen storage densities up to 7 wt% to be achieved as measured by temperature programmed desorption (TPD). We also acquired a new Alexandrite laser and performed initial synthesis experiments which resulted in materials that were ~ 40 - 50 wt% pure SWNTs, in contrast to the 20 - 30 wt% SWNTs typically found in the materials generated with the older laser. Hydrogen storage in carbon single-wall nanotubes is recently becoming the focus of numerous research groups outside of NREL. However, no one has yet achieved the high hydrogen capacities that we have reported. We have therefore this year taken great care to confirm our TPD calibration. We have shown good agreement between our TPD system and our volumetric Seivert's apparatus for three different hydride standards, including Pd, Ti and Ca. In all three cases we observed agreement between the two systems within ± 3% as well as good precision for the expected hydrogen content for each of the samples. Unfortunately, this year we have also found that materials generated with our new Alexandrite laser do not have the high hydrogen storage capacities we reported last year even when all of the same sample purification, cutting and activation steps are taken. Typical hydrogen storage capacities on these new materials range from 2 – 4 wt%. Fortunately however, we have set up our new two color Raman spectroscopy lab which enables us to distinguish between different

types of nanotubes. We have found that our old laser materials were a heterogeneous mixture of both semi-conducting and metallic nanotubes while our new materials contain predominantly metallic tubes. We therefore believe that the semi-conducting tubes may be better suited for hydrogen storage applications. We have performed a very detailed laser-synthesis study of the production of nanotubes versus changing peak pulse power. We have established that semi-conducting tubes are produced at much higher density for very high peak powers. We have also increased our ability to produce tubes with specific diameters. This knowledge will enable us to re-optimize our hydrogen storage capacities on our new materials. Finally, this year we have developed a rapid method for evaluating the purity of a given SWNT material employing Raman spectroscopy at 488 nm.

Statement of the Problem / Relevance of the Work

Background

With the 1990 Clean Air Act and the 1992 Energy Policy Act, the United States recognized the need for a long-term transition strategy to cleaner transportation fuels[1]. This realization comes while the U.S. continues to increase petroleum imports beyond 50% of total oil consumption; with nearly 50% of the total oil consumed being used in the transportation sector[2]. Because of the potential for tremendous adverse environmental, economic, and national security impacts, fossil fuels must be replaced with pollution-free fuels derived from renewable resources. Hydrogen is an ideal candidate as it is available from domestic renewable resources, and usable without pollution. It could therefore provide the long-term solution to the problems created by the Nation's dependence on fossil fuel.

Interest in hydrogen as a fuel has grown dramatically since 1990, and many advances in hydrogen production and utilization technologies have been made. However, hydrogen storage technology must be significantly advanced in performance and cost effectiveness if the U.S. is to establish a hydrogen-based transportation system.

Hydrogen provides more energy than either gasoline or natural gas on a weight basis. It is only when the weight, volume, and round-trip energy costs of the entire fuel storage system and charging/discharging cycle are considered that hydrogen's drawbacks become apparent. New approaches enabling more compact, lightweight, and energy-efficient hydrogen storage are required in order for the wide-spread use of hydrogen powered vehicles to become a reality.

Research and development geared towards implementation of a national hydrogen energy economy has many indirect economic benefits. With almost 600 million vehicles in the world in 1992 - double the number in 1973 - the conflict between energy requirements, power generation, and environmental concerns is felt on a worldwide basis[3]. Thus, in addition to providing domestic energy alternatives, investment in hydrogen energy research will result in opportunities for U.S. technologies in overseas markets.

Currently Available Hydrogen Storage Technologies

Hydrogen can be made available onboard vehicles in containers of compressed or liquefied H_2,

in metal hydrides, or by gas-on-solid adsorption. Hydrogen can also be generated on-board by reaction or decomposition of a hydrogen containing molecular species[4]. Although each method possesses desirable characteristics, no approach satisfies all of the efficiency, size, weight, cost and safety requirements for transportation or utility use. The DOE energy density goals for vehicular hydrogen storage call for systems with 6.5 wt% H_2 and 62 kg H_2/m^3.

Gas-on-solid adsorption is an inherently safe and potentially high energy density hydrogen storage method that should be more energy efficient than either chemical or metal hydrides, and compressed gas storage. Consequently, the hydrogen storage properties of high surface area "activated" carbons have been extensively studied[5-7]. However, activated carbons are ineffective in hydrogen storage systems because only a small fraction of the pores in the typically wide pore-size distribution are small enough to interact strongly with gas-phase hydrogen molecules.

The first measurements of hydrogen adsorption on carbon single-wall nanotubes (SWNTs) were performed here at NREL with highly impure samples. The room-temperature stabilization that was demonstrated at atmospheric pressures suggested the possibility of 5-10 wt % hydrogen storage in SWNT-based systems[8]. Contradictory results from purified SWNTs indicated that such high storage densities could only be achieved with cryogenic temperatures (80 K) and high pressures (158 atm)[9], consistent with theoretical consideration of van der Waals interactions between H_2 and SWNTs[10-12]. However, we showed two years ago that SWNTs can adsorb between 3.5 and 4.5 wt% at room temperature and room pressure when un-optimized preparation procedures were employed, and large-diameter SWNTs were also shown to adsorb 4.2 wt% hydrogen at room temperature and ~100 atm[13]. Last year we showed that hydrogen storage densities can be optimized to values as high as 7 wt%, and presented results from experiments designed to elucidate the mechanisms responsible for the unique hydrogen adsorption properties. There have been various reports of highly different values for SWNT hydrogen storage capacities in the last year from multiple different groups around the world. This "hydrogen storage controversy" was highlighted in a recent report in *Nature* in which our program was cast as leading the field[14]. Due to this extreme controversy, we have taken very careful steps to confirm our measurement calibration this year, and we hope that others in the field will take the same precautions. We have also now believe that semi-conducting single-wall carbon nanotubes have a greater hydrogen storage capacity than metallic tubes. The fact that the types of nanotubes occurring in various materials vary dramatically may account for some of the controversy within the field. Other factors which influence SWNT hydrogen storage capacities of course include sample purity and activation conditions. This year we have developed a laser synthesis method for the production of predominantly semi-conducting tubes and have improved our ability to tailor SWNT diameter distributions. These efforts will enable us to optimize the hydrogen storage properties of the Alexandrite laser materials. We have also developed a method for the rapid determination of whether a given nanotube material is highly pure.

Technical Approach and Summary of Past Work

We have been working on the idea that aligned and self-assembled single wall carbon nanotubes could serve as ideal hydrogen adsorbents since 1993. The concept was motivated by theoretical calculations[15] that suggested that adsorption forces for polarizable molecules within SWNTs would be stronger than for adsorption on ordinary graphite. Thus, high H_2 storage capacities

could be achieved at relatively high temperatures and low pressures as compared to adsorption on activated carbons.

In the Proceedings of the 1994 Hydrogen Program Review, we presented microbalance data that demonstrated gravimetric hydrogen storage densities of up to 8.4 wt% at 82 K and 570 torr on samples containing carbon nanotubes. This substantial uptake at low hydrogen pressures demonstrated the strong interaction between hydrogen and these materials, consistent with higher heats of adsorption than can be found with activated carbons.

In the 1995 Hydrogen Program Review Proceedings, we presented the results of our temperature programmed desorption (TPD) studies that showed significant H_2 adsorption near room temperatures. The adsorption energies on nanotube materials were estimated to be a factor of 2-3 times higher than the maximum that has been observed for hydrogen adsorption on conventional activated carbons. These were the first results which demonstrated the existence of stable adsorbed hydrogen on any type of carbon at temperatures in excess of 285 K. We also analyzed the nanotube production yields versus rod translation rate in the electric arc.

In 1996, we performed a detailed comparative investigation of the hydrogen adsorption properties of SWNT materials, activated carbon, and exfoliated graphite. We also determined that the cobalt nanoparticles present in the arc-generated soots do not play a role in the observed hydrogen uptake. We determined the amount of hydrogen that is stable at near room temperatures on a SWNT basis is between 5 and 10 wt%, and found that an initial heating in vacuum is essential for producing high temperature hydrogen adsorption. Further experiments suggested that SWNTs are selectively opened by oxidation during this heating, and that H_2O is more selective in oxidation than O_2 due to hydrogen termination of dangling bonds at the edges of opened nanotubes. Purposeful oxidation in H_2O resulted in hydrogen storage capacities which were improved by more than a factor of three. We also correlated the measured nanotube densities produced by specific synthesis rod translation rates during arc-discharge with hydrogen storage capacities determined by TPD. Finally, we utilized NREL's High Flux Solar Furnace to form nanotubes by a new and potentially less expensive route for the first time.

In 1997, the desorption of hydrogen was found to fit 1st order kinetics as expected for physisorbed H_2, and the activation energy for desorption was measured to be 19.6 kJ/mol. This value is approximately five times higher than the value expected for desorption of H_2 from planar graphite and demonstrates that SWNT soots can provide very stable environments for H_2 binding. We also employed diffuse reflectance Fourier transform infrared (DRFTIR) spectroscopy to determine the concentrations and identities of chemisorbed species bound to the carbon surface as a function of temperature, and determined that “self-oxidation” allows high-temperature adsorption of hydrogen to occur in the arc-generated SWNT materials. We also began synthesizing SWNT materials in much higher yield than is currently possible with arc-discharge by using a laser vaporization process. We determined that the very long SWNTs made by this method could not be activated towards high-temperature H_2 physisorption by the same oxidative methods that were found to be effective for tubes produced by arc-discharge.

In 1998, we made significant advances in synthesis and characterization of SWNT materials so that we could prepare gram quantities of SWNT samples and measure and control the diameter

distribution of the tubes by varying key parameters during synthesis. By comparing continuous wave (c.w.) and pulsed laser techniques, we learned that it is critical to stay in a vaporization regime in order to generate SWNTs at high yield. We also developed methods that somewhat purified the nanotubes and cut them into shorter segments. We performed temperature programmed desorption spectroscopy on high purity carbon nanotube material obtained from our collaborator Prof. Patrick Bernier, and finished construction of a high precision Seivert's apparatus that allows the hydrogen pressure-temperature-composition phase diagrams to be evaluated for SWNT materials.

In 1999, we improved our laser-based method so that material containing between 20 - 30 wt% SWNTs could be generated at a rate of ~ 150 mg/hr or ~ 1.5 g/day. A simple 3-step purification technique was developed that resulted in single walled carbon nanotubes of greater than 98 wt% purity. A thermal gravimetric analysis (TGA) method was developed to allow the accurate determination of nanotube wt% contents in carbon soots. We also established a process for reproducibly cutting purified laser-generated materials. This advance was necessary since laser-produced tubes were found to be unresponsive to the oxidation methods that successfully opened arc-generated tubes. TPD spectroscopy demonstrated that purified cut SWNTs adsorbed between 3.5 – 4.5 wt% hydrogen under ambient conditions in several minutes and that the adsorbed hydrogen was effectively "capped" by CO_2.

Last year we presented the details of a new cutting procedure and showed that, when optimized, hydrogen storage densities up to 7 wt% can be achieved. Infrared absorption spectroscopy measurements on pristine and H_2-charged samples indicated that no C-H bonds are formed in the hydrogen adsorption process. These experiments are in agreement with an earlier temperature programmed desorption analysis which showed that hydrogen molecules are not dissociated when bound to the SWNT surfaces[8]. This conclusion is further supported by first neutron scattering measurements of hydrogen adsorbed onto SWNTs that were performed through collaboration with researchers at NIST and the University of Pennsylvania[16]. We also developed methods to tune SWNT diameters during synthesis so that mechanistic aspects of H_2 storage could be probed[17], and learned how to de-tangle and organize individual tubes to form "superbundles" that will afford high volumetric storage densities[18]. Finally, we performed the first synthesis experiments with a newly acquired Alexandrite laser. Raman spectroscopy indicated that the as-produced materials were ~ 50 wt% pure SWNTs, in contrast to the 20 to 30 wt% usually seen with the previous laser.

This year we have shown good agreement between our TPD system and our volumetric Seivert's apparatus for three different hydride standards, including Pd, Ti and Ca. In all three cases we observed agreement between the two systems within ± 3% as well as good precision for the expected hydrogen content for each of the samples. Unfortunately, this year we have also found that materials generated with our new Alexandrite laser do not have the high hydrogen storage capacities we reported last year even when all of the same sample purification, cutting and activation steps are taken. Typical hydrogen storage capacities on these new materials range from 2 – 4 wt%. Fortunately, however, we have set up our new two-color Raman spectroscopy lab that enables us to distinguish between different types of nanotubes. We have found that our old laser materials contained a heterogeneous mixture of semi-conducting and metallic nanotubes while our new materials contain predominantly metallic tubes. We have therefore

concluded that the semi-conducting tubes may be better suited for hydrogen storage applications. We have also performed a very detailed laser-synthesis study of the production of nanotubes versus changing peak pulse power. We have established that semi-conducting tubes are produced at much higher density for very high peak powers and increased our ability to produce SWNTs with specific diameters. This knowledge will enable us to re-optimize our hydrogen storage capacities on our new materials. Finally, this year we have developed a rapid method for evaluating the purity of a given SWNT material employing Raman spectroscopy at 488 nm.

Experimental

Pulsed Laser Synthesis of SWNTs

This year the SWNT materials were produced exclusively with our new Alexandrite laser (755 nm). Targets are made by pressing graphite powder doped with 0.6 at% each of Co and Ni in a 1 1/8" inch dye at 20,000 psi. Laser syntheses are performed at 1200 ˚C with 500 Torr Ar flowing at 100 sccm. The laser may be operated in a free-running mode with average powers varying from ~20 - 500 W/cm^2. The free running mode consists of ~ 1 ns pulses that are ≤ 1 ns apart and are produced in packets of ~ 1μs inside a 100 μs train repeated at 10 Hz. The effective pulse width is ~1 μs. For free running laser vaporization, crude soots may be produced at rates of 10-200 mg/hr depending on the laser power density. The Alexandrite laser may also be operated at 10 Hz and a constant average power while the laser pulse width is precisely tuned to a value between 100 ns and 2.5 μs. This capability enables the effect of peak pulse power on SWNT size and type to be unambiguously determined and controlled.

Purification of Laser-generated SWNTs

Approximately 80 mg of the above laser–generated crude is refluxed in 60 ml of 3M HNO_3 for 16 h at 120 °C. The solids are collected on a 0.2 μm polypropylene filter in the form of a mat and rinsed with deionized water. After drying, an ~ 82 wt% yield is obtained. The weight lost is consistent with the digestion of the metal and an additional ~ 12 wt% of the carbon impurities. The carbon mat is then oxidized in stagnant air at 550 ^oC for 10 min., leaving behind pure SWNTs. When care is taken to remain in a vaporization regime during synthesis, materials that are > 98 wt% pure may be obtained as determined by thermal gravimetric analysis (TGA). Also, TGA reveals that since the laser-generated tubes are not highly defective, none of the SWNTs are destroyed in the purification process.

Cutting of Laser-generated SWNTs

Purified 1-3 mg samples are sonicated in 20 ml of 4M HNO_3 with a high-energy probe for 10 minutes to 24 hrs at powers ranging from 25 – 250 W/cm^2. The very long nanotube ropes found after purification[19] are cut and re-assembled. This large-scale cutting observed is consistent with the generation of cuts and defects that have been observed by others[20-22]. We find that cutting with a high-energy probe in HNO_3 is necessary to achieve high-capacity ambient H_2 adsorption.[9] Also the cutting process incorporates metal particles ranging in size from several nanometers to several microns in the SWNT samples. X-ray patterns of the particles in the cut samples are consistent with an alloy of nominal composition $TiAl_{0.1}V_{0.04}$ as expected for disintegration of the

ultrasonic probe. We believe that this alloy mediates the hydrogen adsorption process and is necessary to observe high hydrogen storage capacities.

Temperature Programmed Desorption

Details of the ultra high vacuum (UHV) chamber employed for the TPD studies have been reported previously[4,8]. Briefly, carbon samples weighing ~1 mg are placed in a packet formed from 25 μm thick platinum foil and mounted at the bottom of a liquid nitrogen cooled cryostat. The packet is resistively heated with a programmable power supply. Pinholes in the foil enable gas diffusion into and out of the packet. An ion gauge and capacitance manometer are employed to monitor pressure. Gas exposures are controlled with a variable conductance leak valve. Isolation gate valves separate the sample compartment during high-pressure gas exposures. A mass spectrometer measures species with an m/e up to 300 a.m.u. and insures that only hydrogen is involved in adsorption/desorption cycles. The instrument is easily calibrated[23] by thermally decomposing known amounts of CaH_2. The amount of evolved hydrogen is linear with the weight of decomposed CaH_2, and the calibrations were performed with amounts of CaH_2 that yield a TPD signal similar to the SWNT samples. The TPD system has also been calibrated with hydrogen desorption studies of Pd and Ti hydrides. All three hydrogen calibration methods have been confirmed with our Seivert's volumetric technique within ±3%. Prior to hydrogen adsorption studies SWNT samples are initially degassed by heating in a vacuum of ~ 10^{-7} torr to 823 - 973 K at 1 K/s. The sample temperature is measured with a thin thermocouple spot-welded to the platinum packet. Room temperature H_2 exposures for ~ 1 minute at pressures between 10–500 torr saturate the hydrogen adsorption. Capacity determinations in the TPD are done by cooling the sample to 130 K prior to evacuation of the chamber.

Raman Spectroscopy

Raman spectroscopy is performed using ~7 mW of the 488 nm line of an Ar ion laser or ~9 mW of the 632.8 nm line of a HeNe laser. The scattered light is analyzed with a Jobin Yvon 270M spectrometer equipped with a liquid-nitrogen cooled Spectrum One CCD and a holographic notch filter. A 2400 grooves/mm grating is employed at 488 nm. However, it is necessary to employ a 1200 grooves/mm grating at 632.8 nm in order to observe the entire spectral range of interest. A Nikon 55 mm camera lens is employed both to focus the beam on the sample to a ~0.25 mm^2 spot and to collect the Raman scattered light. At 488 nm a resolution of 2-4 cm^{-1} was measured across the entire range with Oriel spectral calibration lamps. The resolution is decreased by approximately a factor of two for the spectra obtained at 632.8 nm. Averaging three 30 s scans is sufficient to obtain high intensity, well-resolved Raman spectra. Raman spectra are normalized for the different laser powers.

Seivert's Apparatus

The schematic diagram of the volumetric (Sievert's) apparatus is shown in Figure 1. The amount of H_2 gas adsorbed in a test sample is determined by measuring the pressure of a known number of gas moles introduced into a calibrated volume at known temperature as a function of time. Helium gas is used to calibrate the sample volume including the dead space of the sample itself. The total amount of hydrogen adsorbed can also be measured through desorption.

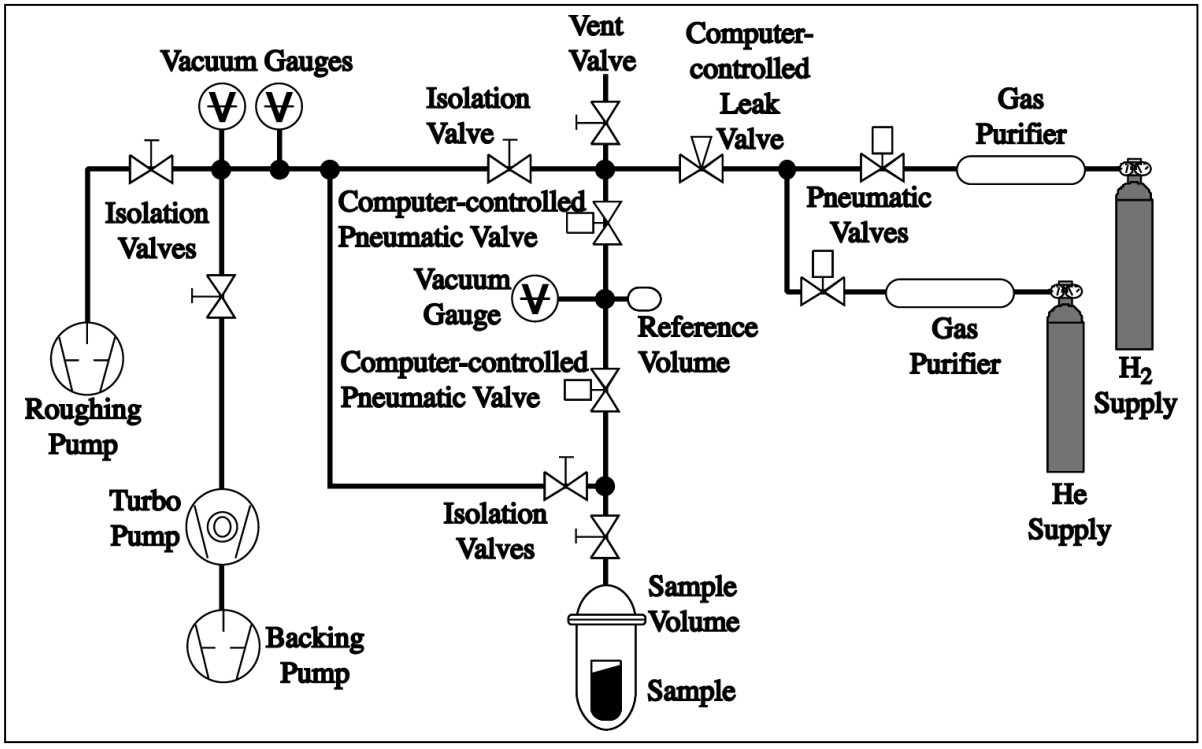

Figure 1: Schematic diagram of the Seivert's volumetric apparatus.

Results and Discussion

Rigorous Calibration of TPD Apparatus

Figure 2 displays temperature programmed desorption curves for the three standards employed to calibrate the TPD system including a) calcium hydride, b) palladium hydride and c) titanium hydride. Several separate spectra were obtained following the same sample preparation technique for a given hydride, and very good agreement is obtained in each case. The CaH_2 was employed to establish the initial sensitivity of the TPD mass spectrometer. It was assumed that the 95 wt% pure Aldrich CaH_2 supplies a standard which is 4.5 wt% hydrogen, a value similar to the capacities observed for our SWNT samples. This type of approach has been used successfully by others to achieve good accuracy calibrating systems for CO_2 desorption[23]. We have also directly measured the hydrogen desorption for a CaH_2 sample that has been completely decomposed in our Seivert's apparatus to correspond to a value of 4.35 wt%.

In an effort to further solidify our TPD calibration, we endeavored to find a standard that could be charged *in situ* with identical pressure/temperature cycling and analyzed by both the TPD and Seivert's methods. Ideally, we would be able to perform the calibration with a pressure/temperature cycle which was similar to that used for charging SWNT samples. Palladium powder was chosen since fast hydrogen adsorption/desorption kinetics can be obtained at relatively low temperatures, and well-defined capacities of hydrogen can be repeatedly prepared. We first obtained adsorption isotherms from a Pd sample with the Seivert's

apparatus. Figure 3 shows an adsorption isotherm obtained from a Pd sample at 28 °C. The curve is in good agreement with adsorption isotherms published in the literature[24], showing a knee in the curve at 0.65 H/M. To evaluate the H/M value at lower temperatures, the Pd was charged with 20 torr H_2 at room temperature and then cooled with liquid nitrogen. While the sample was cooled, the head-space gas was evacuated. The sample was then heated to 300 °C and the trapped hydrogen was desorbed into the closed system. The number of moles of gas evolved was determined by measuring the pressure rise in the closed system after accounting for the fact that a small portion of the system volume was at 300 °C (the remainder being at 28 °C). Separate experiments confirmed that additional hydrogen uptake did occur while the sample was cooled from room temperature, and that the kinetics of hydrogen adsorption/desorption were "frozen-out" at ~120 K. The H/M value for the Pd after this P-T cycle was found to be 0.77 to 0.79 as expected from the literature[25]. Palladium samples were then loaded into the TPD apparatus, and the same P-T charging cycle was performed. Following temperature programmed desorption, the integrated area of the TPD curve indicated an amount of hydrogen equal to 0.78 H/M using the calibration value determined from the CaH_2 decomposition experiments. Thus, good agreement was found between the TPD and Seivert's systems when cross-calibration was performed using a well-behaved standard charged under identical conditions.

As a final calibration test we monitored the hydrogen desorption from a TiH_2 standard obtained from our CRADA partners, Honda R & D Americas, Inc.. The titanium hydride was assumed to be charged to the maximum capacity of 4 wt% hydrogen. A value of exactly 4.0 wt% was measured for this

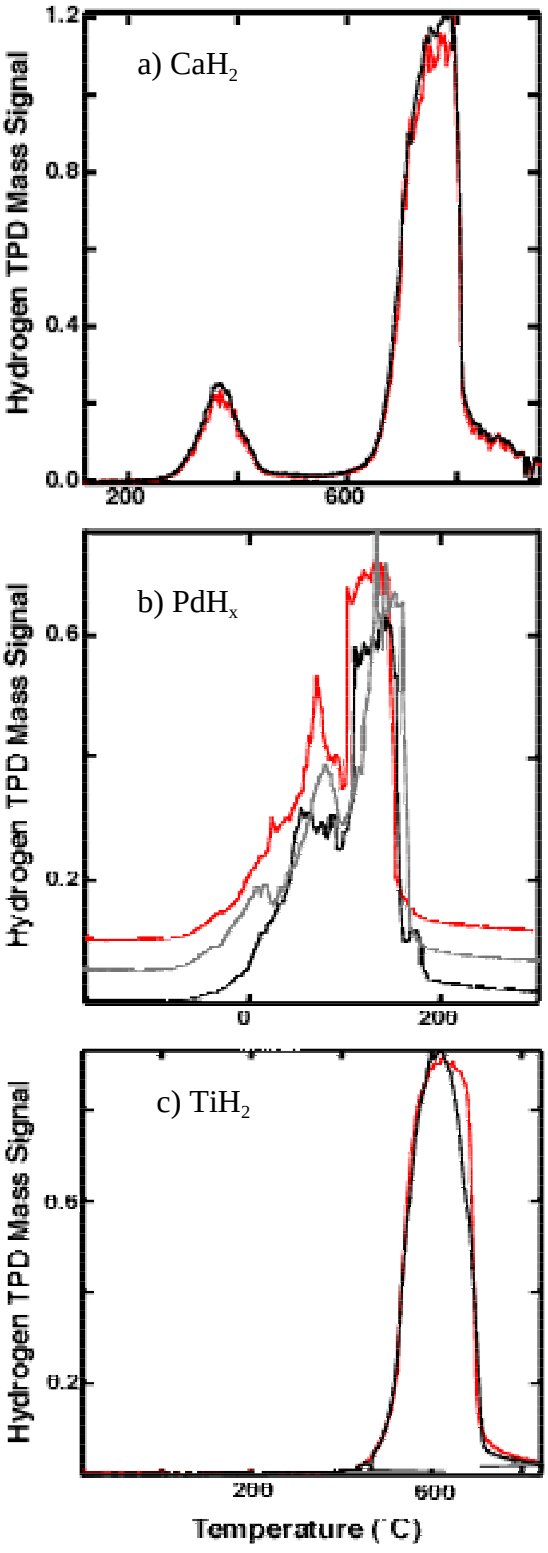

Figure 2: Hydrogen TPD spectra for three different calibration standards: a) CaH_2, b) PdH_2 and c) TiH_2.

standard with our volumetric technique, and employing the TPD technique a value of 3.9 wt% was obtained. Following these very careful calibration efforts, we are supremely confident in all of our reported SWNT hydrogen storage capacities. Since the development of a high capacity hydrogen storage system is so extremely important to the utility of hydrogen as a renewable energy source, we hope that all of the research groups working in the area will also take great care in reporting very accurate hydrogen adsorption measurements.

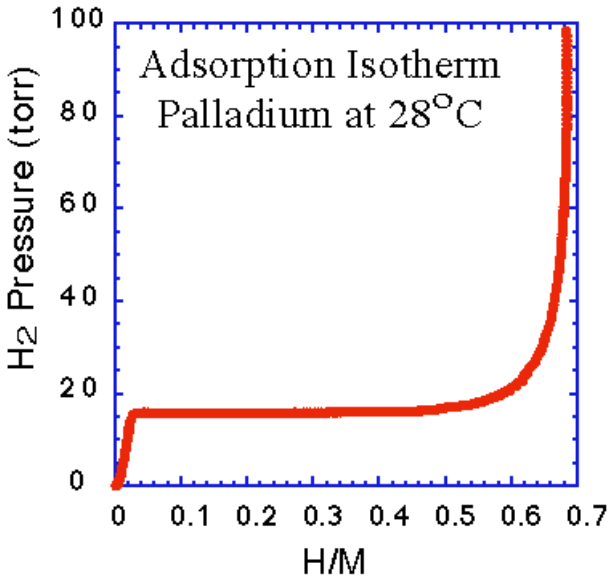

Figure 3: Adsorption isotherm from Pd sample at 28 °C, showing a knee in the curve at 0.65 H/M.

Decreased Hydrogen Adsorption on Alexandrite Laser Materials

By the end of the last fiscal year, the Molectron Nd:YAG laser that was in use to produce our SWNT materials had been failing more and more regularly. Additionally problematic was the fact that the laser spot itself was very inhomogeneous and irreproducible after required flash lamp changes. We therefore replaced the Molectron with a new Light Age, Inc., Alexandrite laser. Raman spectroscopy indicated that the as-produced materials were ~ 40 to 50 wt% pure SWNTs, in contrast to the 20 to 30 wt% usually seen with the Molectron laser. However, following our standard purification, cutting and activation techniques, we found that the hydrogen storage capacities of the Alexandrite laser generated materials were typically between 2.0 – 4.0 wt%. Figure 4a displays a typical TPD spectrum of an Alexandrite laser generated material. This particular sample capacity was measured at 3.5 wt%. As observed previously hydrogen desorption occurs from at least two desorption sites with TPD peaks at ~410 and ~613 K. Figure 4b displays the desorption isotherm obtained with our Seivert's apparatus for the same sample. Here a value of only 2.5 wt% hydrogen was measured.

In general we have found the hydrogen adsorption capacities of SWNT materials measured with our Seivert's apparatus to be ~40-50 wt% lower than the values obtained with our TPD apparatus. We believe that the lower hydrogen capacities are measured for SWNT samples in the Seivert's system because there is an inherent difference in the way samples are degassed. In the Seivert's apparatus the dimensions of the tubing are small, as is the case for most volumetric systems. It is therefore impossible to degas the sample as efficiently as in the TPD system which has very high conductance. This failure to fully degas the sample results in a reduced hydrogen storage capacity. It is also apparent that the hydrogen storage capacities for the Alexandrite materials have decreased significantly from the values of 6-7 wt% reported last year for the Nd:YAG materials. These results suggest that the type of SWNT employed for various adsorption materials may be very critical to the optimization of hydrogen storage capacities. Thus, since we have shown that both SWNT type and subsequent processing are critical to

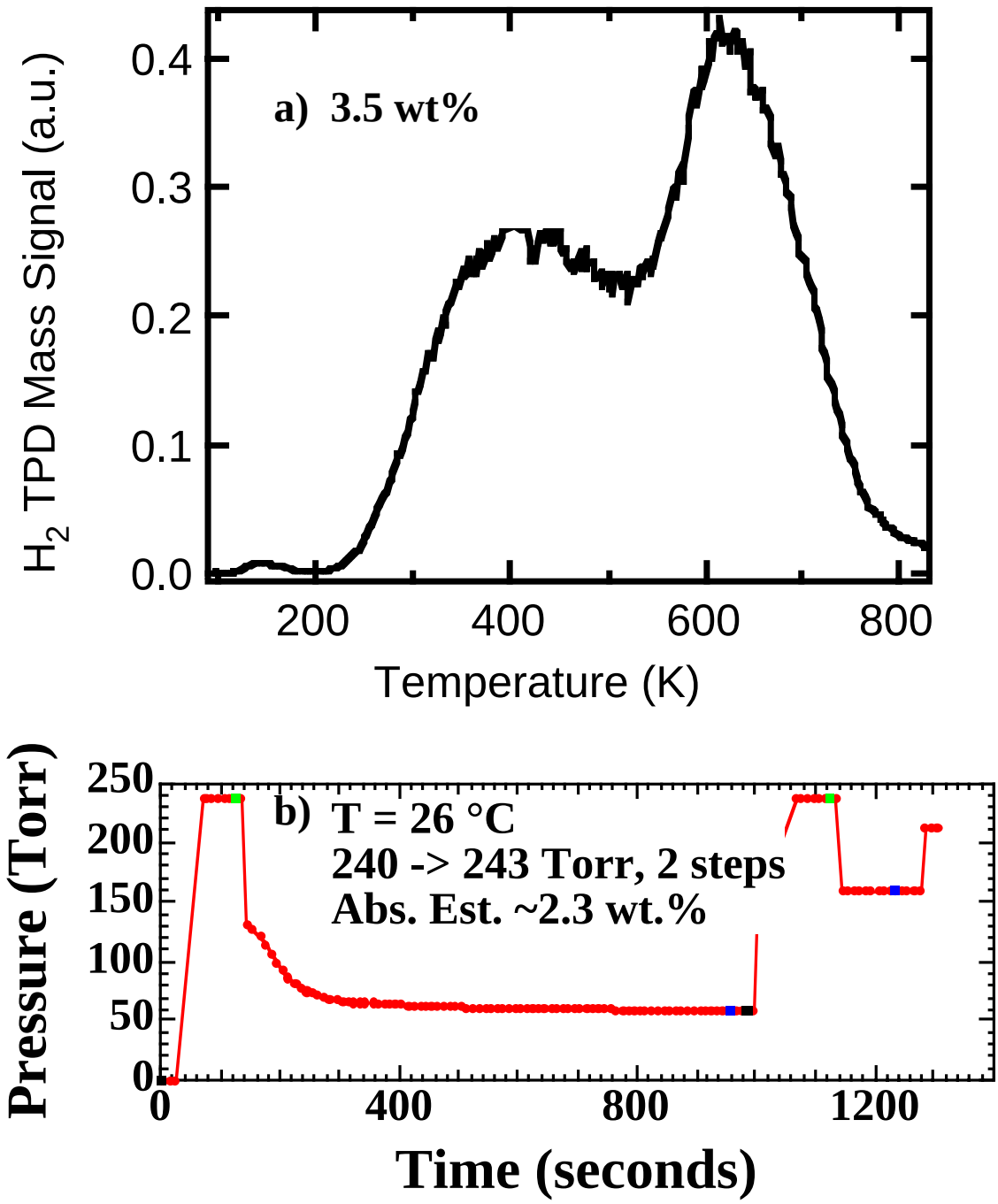

Figure 4: Hydrogen desorption from an Alexandrite laser generated material as probed by a) temperature programmed desorption and b) the Seivert's volumetric apparatus. The measured hydrogen capacities were 3.5 wt% and 2.5 wt%, respectively. The lower value measured by the Seivert's apparatus is attributed to difficulty in degassing the sample efficiently in the volumetric apparatus.

optimizing hydrogen storage properties, the large discrepancies reported for hydrogen storage on various carbon nanotube materials are perhaps not unanticipated.

Optimal Nanotubes for Hydrogen Storage and Their Controlled Laser Production

We have recently acquired a He:Ne (632.8 nm) laser for our Raman spectroscopy set-up. Previously the system relied upon a single Ar ion laser (488 nm). The Raman modes of SWNTs are resonantly enhanced with different tubes being at resonance for different wavelengths of excitation. At 488 nm only semi-conducting SWNTs are at resonance resulting in a Raman signal that is essentially due to resonant semi-conducting tubes. At 632.8 nm both metallic and semi-conducting nanotubes may be at resonance[26]. However, the dominant peaks of the Raman tangential bands for semi-conducting SWNTs occur at 1563 and 1591 cm^{-1} while those for the metallic tubes occur at 1540 and 1581cm^{-1}[26]. Figure 5 displays the Raman spectra in the radial breathing mode region of a) Nd:YAG and b) Alexandrite laser-generated crude materials for excitations at 488 and 632.8 nm. The frequencies observed for the SWNT radial breathing modes are strongly diameter-dependent with the smaller tubes appearing at higher frequency[27]. For both of these materials the tangential bands observed for 632.8 nm were not significantly shifted from the values reported for the dominant peaks of the metallic tubes. It may therefore be assumed that predominantly metallic SWNTs are being probed for these laser-generated materials[28].

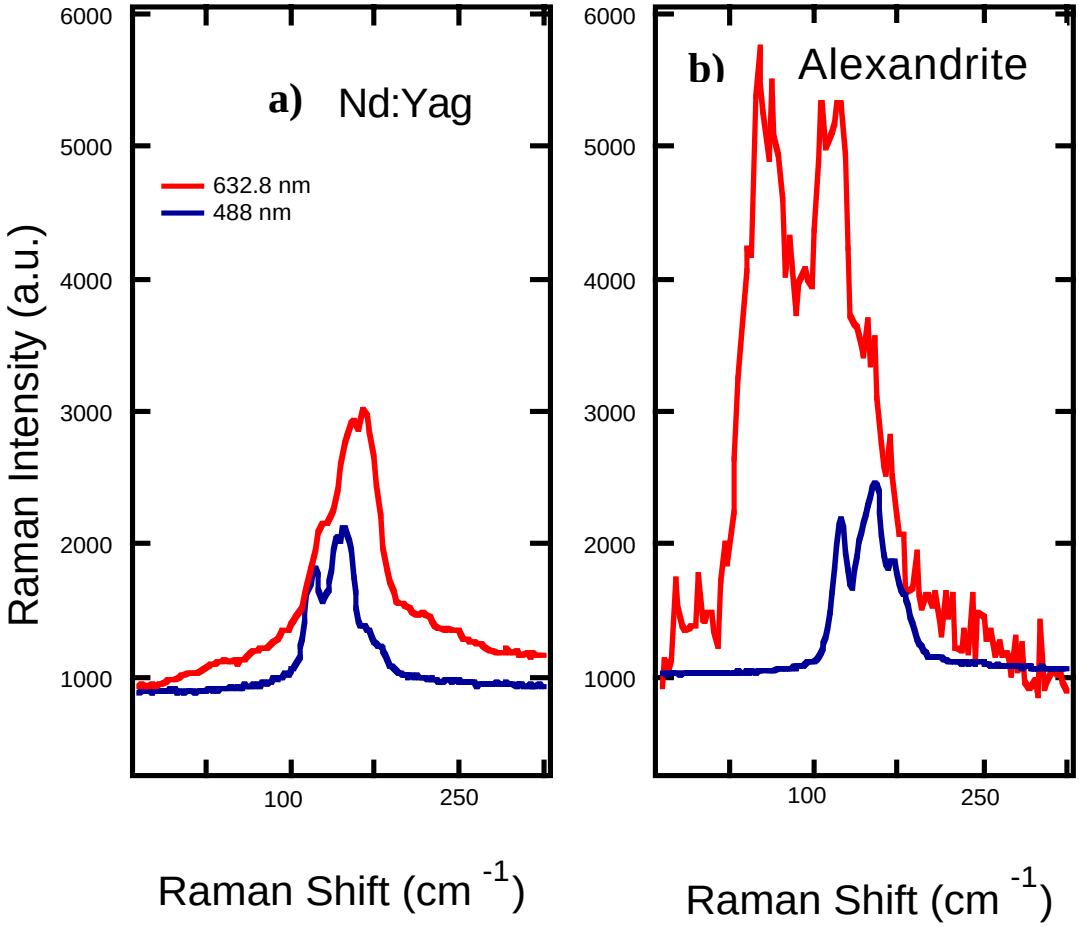

Figure 5: Raman spectra of the radial breathing modes for excitations at 488 and 632.8 nm of laser generated materials generated with a) the Nd:YAG and b) the Alexandrite.

The spectra of the radial breath modes for the Nd:YAG and Alexandrite materials appear quite different. The most striking feature is that the intensity of the spectrum observed at 632.8 nm in Fig 5b is much stronger relative to that observed at 488 nm implying a much larger concentration of metallic tubes in the Alexandrite materials. Since the hydrogen storage capacities for the Alexandrite materials have decreased from 6-7 wt% (Nd:YAG) to 2-4 wt%, the Raman results also suggest that semi-conducting single-wall carbon nanotubes are more efficient for the optimization of hydrogen storage capacity. We have therefore conducted a very detailed study of the production of specific sizes and types of SWNTs versus laser peak pulse power employing the Alexandrite laser[28]. We have found that at a constant synthesis temperature of 1200 ˚C, the diameter distributions of both the semi-conducting and the metallic SWNTs may be tailored through variation in laser peak pulse power. In each case smaller diameter nanotubes are produced with increasing peak pulse power. It is also possible to regulate the fractions of the semi-conducting or metallic tubes by varying the synthesis peak pulse power. In this case, higher peak powers result in the production of semi-conducting SWNTs at a much higher density. It is possible that not only the ratio of the semi-conducting to metallic SWNTs is important for the optimization of hydrogen storage properties but also that the production of the specific diameters observed in Fig. 5a is critical for optimal hydrogen adsorption. In either case we are well poised to tailor the nanotube contents of our Alexandrite materials and obtain an optimal hydrogen storage capacity that equals or exceeds that observed for the Nd:YAG materials.

A Simple Method to Determine if SWNT Materials Contain Carbon Impurities

In 1999, we developed a rigorous method for the determination of SWNT contents in various materials employing thermal gravimetric analysis (TGA) and inductively coupled plasma spectroscopy[19]. It is often desirable though to obtain a more rapid estimate of whether a given nanotube material is high quality. However, we have found that employing other commonly used analytical tools to estimate SWNT contents in various materials can sometimes be misleading. For example Fig. 6a displays a scanning electron microscope (SEM) image of crude laser-generated material. In the SEM image it is very difficult to discern any non-nanotube fractions in the material either carbon or metal. The SEM image therefore suggests that this crude laser-generated material is perhaps greater than 90 wt.% SWNTs. Figure 6b, however, is a TEM image of the same nanotube crude. In this image the single-wall carbon nanotubes are still readily apparent, but amorphous carbon and/or nano-crystalline graphite as well as metal nanoparticles are also easily observed. Although TGA analysis of this material following a nitric acid reflux showed this material to be high quality, containing ~35wt.% SWNTs, it is obviously not nearly as pure as the SEM image of Fig. 6a suggests. Figure 6 indicates that transmission electron microscopy is a more powerful technique for determining SWNT purity levels than scanning electron microscopy. However, employing TEM to estimate SWNT purity levels is still not sufficient. The most obvious reason is simply that TEM is a highly localized technique. While one section on a TEM grid may appear to contain only carbon nanotubes, another could depict micron sized particles of graphite. In addition, it is very difficult to tell from a TEM image of nanotube bundles whether the tubes are surrounded by an impurity coating. Such a coating could easily constitute as much as 50 wt.% of the material.

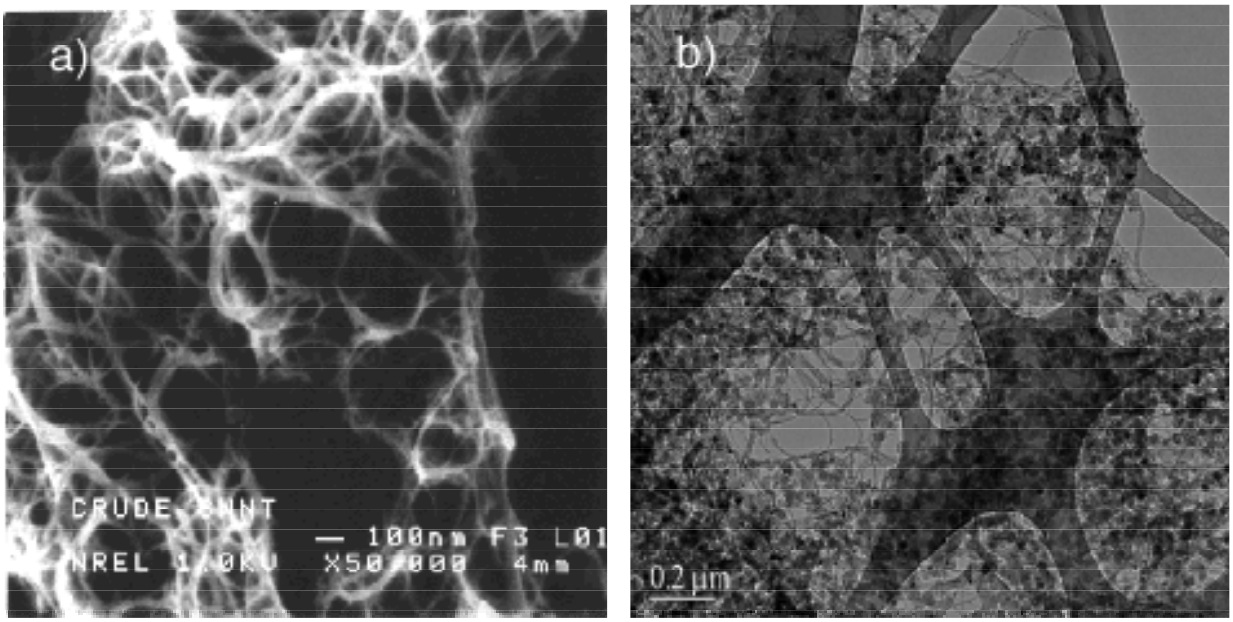

Figure 6: a) SEM image of laser generated SWNT crude and **b)** TEM image of the same material. Although this material contains only ~35 wt.% SWNTs, the SEM image is similar to SEM images observed for materials that contain > 90 wt.% SWNTs.

We have established a method using Raman spectroscopy to determine whether the non-nanotube carbon fractions have been removed during purification[29]. Figure 7a displays Raman spectra of the tangential modes of a laser-generated crude and of the same material following purification. As expected the intensity of the spectrum of the purified material is greater than that of the spectrum of the impure sample. However, it is not possible to correlate Raman intensity to absolute purity of the SWNT samples as the intensities of fully purified materials vary dramatically. This is likely simply due to the presence of different concentrations of SWNTs that are resonantly enhanced at the particular excitation wavelength[27]. A blow-up of the Raman spectra of the crude and purified materials is shown in Fig. 7b. Here the SWNT Raman band at 1350 cm^{-1} is clearly observed. It is striking that the band for the purified material is much narrower than the band for the crude. This is because the band of the crude material is also comprised of the much broader D-band of nanocrystalline graphite impurities. We have found that for purified SWNT samples that are free of non-nanotube carbon, the ratios of the SWNT band at 1593 cm^{-1} to the band at 1350 cm^{-1} are constant for both the heights and the full-widths-at-half-maximums. The ratio of the area of the band at 1350 cm^{-1} to the area of all three[27] of the tangential bands is also constant. If all three of these conditions are met, Raman spectroscopy identifies the SWNT samples as being free of non-nanotube carbon impurities. Unfortunately Raman spectroscopy is blind to the presence of residual metal catalyst particles. TGA and ICP allow this fraction to be quantified. Also the values of the ratios may not be extrapolated to estimate SWNT contents in impure materials as the widths of the impurity D-bands vary as a function of the particle size. However, this ability to rapidly determine whether a given single-wall carbon nanotube sample is free from carbon impurities should facilitate the wide array of SWNT research efforts including the development of a carbon nanotube based vehicular hydrogen storage system.

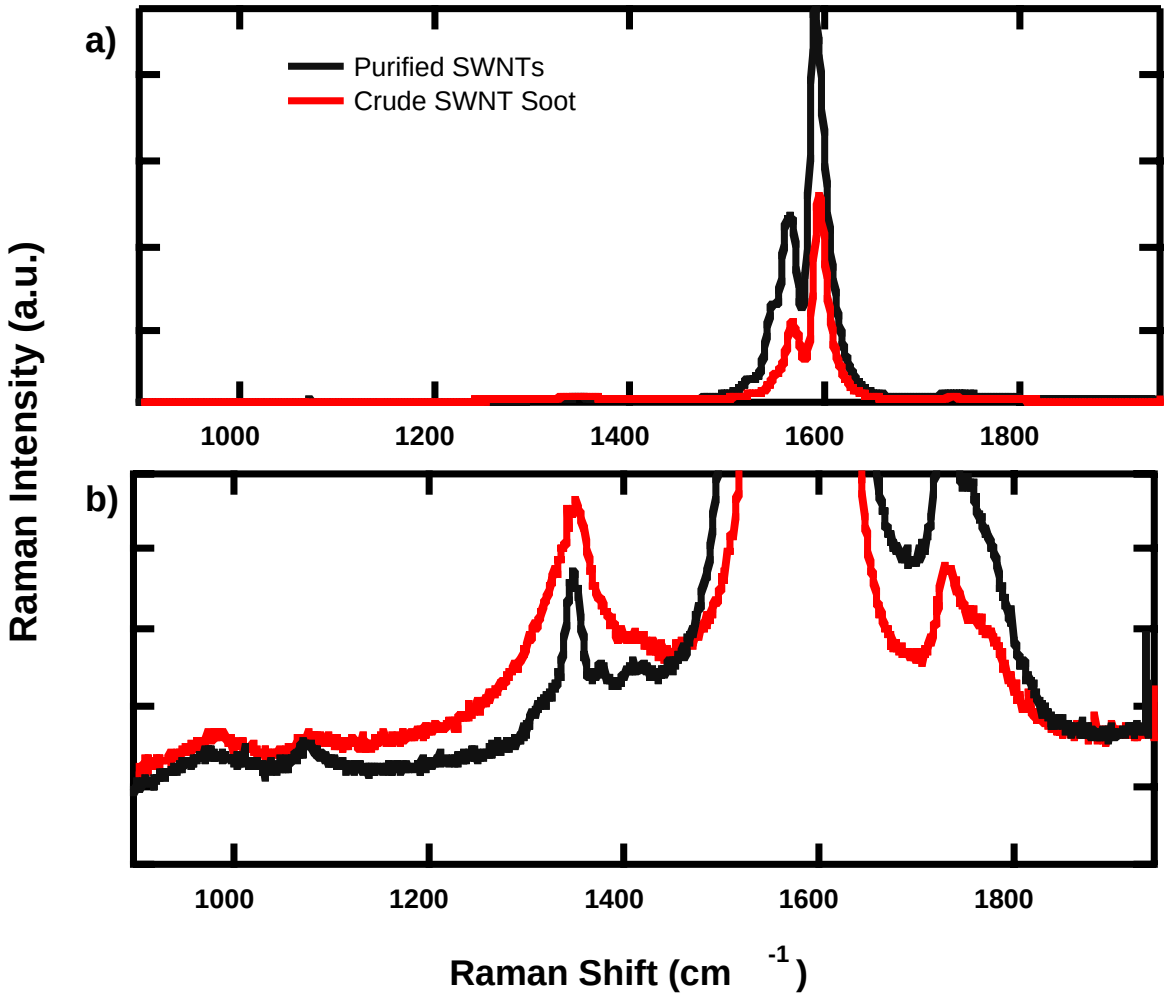

Figure 7 : Raman spectra of **a)** crude and purified laser-generated SWNTs between 1000-1800 cm^{-1} and **b**) a blow-up of the same spectra to magnify the band at 1350 cm^{-1}.

Conclusions/Future Work

Hydrogen storage in carbon single-wall nanotubes is recently becoming the focus of numerous research groups outside of NREL. In fact we were recently highlighted as the field leaders in a *Nature* article focusing on the wide scope of reported hydrogen storage capacities in carbon single-wall nanotube materials[14]. Because a such a wide-range of SWNT hydrogen storage capacities has been reported, we have taken great care to confirm our TPD calibration. We have shown good agreement between our TPD system and our volumetric Seivert's apparatus for three different hydride standards, including Pd, Ti and Ca. In all three cases we observed agreement between the two systems within ± 3% as well as good precision for the expected hydrogen content for each of the samples. We therefore have utmost confidence in all of the hydrogen storage numbers that we report. We hope that other groups will take care to ensure the accuracy of their measurements as well.

Unfortunately, this year we have also found that materials generated with our new Alexandrite laser do not have the high hydrogen storage capacities we reported last year even when all of the same sample purification, cutting and activation steps are taken. Typical hydrogen storage capacities on these new materials range from 2 – 4 wt%. Fortunately however, we have set up our new two color Raman spectroscopy lab that enables us to distinguish between different types of nanotubes. We have found that our old laser materials were a heterogeneous mixture of both semi-conducting and metallic nanotubes while our new materials contain predominantly metallic tubes. We therefore believe that the semi-conducting tubes may be more optimal for hydrogen storage applications.

We have performed a very detailed laser-synthesis study with our new Alexandrite laser on the production of nanotubes versus changing peak pulse power. We have found that at a constant synthesis temperature of 1200 ˚C, the diameter distributions of both the semi-conducting and the metallic SWNTs may be tailored through variation in laser peak power. In each case smaller diameter nanotubes are produced with increasing peak pulse power. It is also possible to regulate the fractions of the semi-conducting or metallic tubes by varying the synthesis peak pulse power. Here, higher peak powers result in the production of semi-conducting SWNTs at a much higher density.

Finally we have developed a simple method employing Raman spectroscopy at 488 nm to determine the presence of carbon impurities in SWNT materials. This process enables us to quickly identify high purity SWNT samples. The new capability will greatly facilitate our hydrogen storage research efforts.

The fact that we have increased our synthesis capabilities to produce SWNTs with both specific sizes and types should enable us to fully optimize a SWNT hydrogen storage system. Our discovery this year that the Alexandrite laser generated materials have reduced storage capacities and also contain predominantly metallic SWNTs suggests that semi-conducting SWNTs are more effective for hydrogen storage applications. It may also be possible that hydrogen storage is only optimized for a very specific and narrow diameter range of SWNTs. In the upcoming year we will continue to evaluate the most optimal tube composition for hydrogen storage applications. We will then employ our new Alexandrite controlled production methods to produce these refined materials. Our current state of the art production and purification techniques provide gram quantities of high quality material per day. We will of course continue to focus on up-scaling the production and purification of SWNT adsorbent materials.

Acknowledgements

T. Gennett worked at NREL while under a sub-contract to Rochester Institute of Technology. We wish to thank Leonid Grigorian from Honda R&D Americas for many helpful conversations.

References

1 J. S. Cannon, *Harnessing Hydrogen* (INFORM, Inc., New York, 1995).
2 National Energy Strategy (1991/1992).

3 C. Flavin and N. Lessen, *Power Surge* (W.W. Norton & Co., New York, 1994).
4 A. C. Dillon, T. A. Bekkedahl, A. F. Cahill, K. M. Jones, and M. J. Heben, in *Carbon Nanotube Materials for Hydrogen Storage*, Coral Gables, FL, 1995, p. 521-542.
5 C. Carpetis and W. Peschka, Int. J. Hydrogen Energy 5, 539-554 (1980).
6 J. A. Schwarz, in *Modification Assisted Cold Storage (MACS)*.
7 J. A. Schwarz, in *Activated Carbon Based Storage System*, Honolulu, HI., 1992, p. 271-278.
8 A. C. Dillon, K. M. Jones, T. A. Bekkedahl, C. H. Kiang, D. S. Bethune, and M. J. Heben, Nature **386,** 377-379 (1997).
9 Y. Ye, C. C. Ahn, C. Witham, B. Fultz, J. Liu, A. G. Rinzler, D. Colbert, K. A. Smith, and R. E. Smalley, Applied Physics Letters **74,** 2307 (1999).
10 Q. Wang and J. K. Johnson, J. Phys. Chem. B **103,** 4809-4813 (1999).
11 Q. Wang and J. K. Johnson, J. Chem Phys. B **110,** 577-586 (1999).
12 M. Rzepka, P. Lamp, and M. A. d. l. Casa-Lillo, J.Phys. Chem **102,** 10894-10898 (1998).
13 C. Liu, Y. Y. Fan, M. Liu, H. T. Cong, H. M. Cheng, and M. S. Dresselhaus, Science **286,** 1127 (1999).
14 C. Zandonella, Nature **410,** 734-5 (2001).
15 M. R. Pederson and J. Q. Broughton, Physical Review Letters **69,** 2689 (1992).
16 C. M. Brown, T. Yildirim, D. A. Neuman, M. J. Heben, T. Gennett, A. C. Dillon, J. L. Alleman, and J. E. Fischer, Chem. Phys. Lett. **329**, 311-316 (2000).
17 A. C. Dillon, P. A. Parilla, J. L. Alleman, J. D. Perkins, and M. J. Heben, Chem. Phys. Lett. **316,** 13-18 (2000).
18 T. Gennett, A. C. Dillon, J. L. Alleman, F. S. Hassoon, K. M. Jones, and M. J. Heben, Chem. of Mat. **12,** 599-601 (2000).
19 A. C. Dillon, T. Gennett, K. M. Jones, J. L. Alleman, P. A. Parilla, and M. J. Heben, Advanced Materials **11,** 1354-1358 (1999).
20 K. B. Shelimov, R. O. Esenaliev, A. G. Rinzler, C. B. Huffman, and R. E. Smalley, Chem. Phys. Lett. **282,** 429-34 (1998).
21 J. Liu, A. G. Rinzler, H. Dai, J. H. Hafner, K. R. Bradley, P. J. Boul, A. Lu, T. Iverson, K. Shelimov, C. B. Huffman, F. Roderiguez-Macias, Y.-S. Shon, T. R. Lee, D. T. Colbert, and R. E. Smalley, Science **280,** 1253-56 (1998).
22 K. L. Lu, R. M. Lago, Y. K. Chen, M. L. H. Green, P. J. F. Harris, and S. C. Tsang, Carbon **34,** 814-16 (1996).
23 J. Wang and B. McEnaney, Thermochimica Acta. **190,** 143-153 (1991).
24 H. Frieske, E.Wicke, and B. Bunsenge, Physik Chem **77,** 50 (1973).
25 Schirber and Northrup, Phys. Rev. B **10,** 3818 (1974).
26 P. Pimenta, M. Marucci, S. D. M. Brown, M. J. Matthews, A. M. Rao, P. C. Eklund, R. E. Smalley, G. Dresselhaus, and M. S. Dresselhaus, Journal of Materials Research **13,** 2396-2403 (1998).
27 A. M. Rao, E. Richter, S. Bandow, B. Chase, P. C. Eklund, K. A. Williams, S. Fang, K. R. Subbaswamy, M. Menon, A. Thess, R. E. Smalley, G. Dresselhaus, and M. S. Dresselhaus, Science **275,** 187-191 (1997).
28 A. C. Dillon, J. L. Alleman, T. Gennett†, K. M. Jones, P. Parilla, K. E. H. Gilbert, and M. J. Heben, (submitted to J. Phys. Chem.).
29 A. C. Dillon, T. Gennett, J. L. Alleman, K. M. Jones, P. Parilla, and M. J. Heben, (submitted to Appl. Phys. Lett.).